

Three-wave interactions and spatio-temporal chaos

A. M. Rucklidge

Department of Applied Mathematics, University of Leeds, Leeds LS2 9JT, UK

M. Silber

*Department of Engineering Sciences and Applied Mathematics,
and NICO, Northwestern University, Evanston, IL 60208, USA*

A. C. Skeldon

Department of Mathematics, University of Surrey, Guildford GU2 7XH, UK

(Dated: 2 November 2011)

Three-wave interactions form the basis of our understanding of many pattern forming systems because they encapsulate the most basic nonlinear interactions. In problems with two comparable length scales, it is possible for two waves of the shorter wavelength to interact with one wave of the longer, as well as for two waves of the longer wavelength to interact with one wave of the shorter. Consideration of both types of three-wave interactions can generically explain the presence of complex patterns and spatio-temporal chaos. Two length scales arise naturally in the Faraday wave experiment with multi-frequency forcing, and our results enable some previously unexplained experimental observations of spatio-temporal chaos to be interpreted in a new light. Our predictions are illustrated with numerical simulations of a model partial differential equation.

PACS numbers: 47.54.-r, 47.52.+j, 05.45.-a, 47.35.Pq

Patterns arise in many non-equilibrium physical, chemical and biological systems, often when a uniform state is subjected to external driving and becomes unstable to modes with a finite wavelength. In some systems, modes with a second wavelength can play an important role in pattern formation if these modes are either unstable or only weakly damped. The interaction between two waves of one wavelength with a third wave of the other wavelength is known both experimentally and theoretically to play a key role in producing a rich variety of interesting phenomena such as quasipatterns, superlattice patterns and spatio-temporal chaos (STC) [1–8].

In this paper, we focus on three-wave interactions (3WIs) involving two comparable wavelengths and develop a criterion for when such interactions are likely to lead to STC, as opposed to steady patterns and quasipatterns. The mechanism we describe is generic, and will apply to any system in which such 3WIs can occur, such as the Faraday wave experiment [1–3], coupled Turing systems [4] and some optical systems [5]. In order to illustrate our criterion we focus on two examples. The first is the Faraday experiment, in which patterns of standing waves are excited on the surface of a fluid by periodically forcing the fluids' container up and down. Using a multi-component forcing $f(t)$ enables the excitation of waves with comparable wavelengths. Experimentally, the phases and amplitudes of the different components of $f(t)$ have been shown to determine whether simple patterns, superlattice patterns, quasipatterns or STC are seen [1–3]. A theoretical understanding of the stabilization of some superlattice patterns has been developed using a single 3WI [2, 6, 7], but up until this point there has been no explanation for the presence of STC. We show how our extension of the notion of 3WIs can explain the

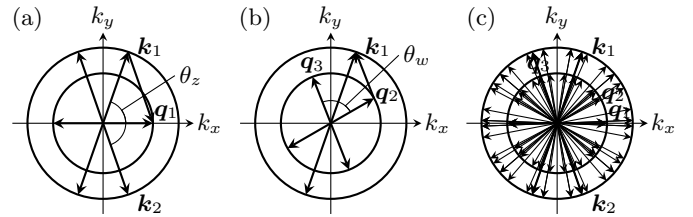


FIG. 1: Three-wave interactions between waves on two critical circles, with outer radius 1 and inner radius $q > \frac{1}{2}$. (a) A vector \mathbf{q}_1 on the inner circle can be written as the sum of two vectors \mathbf{k}_1 and \mathbf{k}_2 on the outer circle; this defines the angle $\theta_z = 2 \arccos(q/2)$. (b) The vector \mathbf{k}_1 is the sum of two inner vectors \mathbf{q}_2 and \mathbf{q}_3 ; this defines the angle $\theta_w = 2 \arccos(1/2q)$. (c) Similarly, \mathbf{k}_2 is the sum of two inner vectors, and each of these is in turn the sum of two outer vectors, and so on.

origin of STC, quasipatterns and other features of the experimental results of [3]. Our second example is a new model PDE that has been designed to enable an exploration of 3WIs with two comparable wavelengths.

We suppose that in the system two wavenumbers $k = 1$ and $k = q$ are excited with $0 < q < 1$. 3WIs then can take two forms: first, two waves on the outer circle (wavenumber 1) interact nonlinearly with a wave on the inner circle (wavenumber q), for example \mathbf{k}_1 and \mathbf{k}_2 with $\mathbf{q}_1 = \mathbf{k}_1 + \mathbf{k}_2$ (figure 1a); and second, if $\frac{1}{2} < q < 1$, two waves on the inner circle interact with one on the outer circle, for example vectors \mathbf{q}_2 and \mathbf{q}_3 with $\mathbf{k}_1 = \mathbf{q}_2 + \mathbf{q}_3$ (figure 1b). The consequence of the presence of both forms of interaction when $\frac{1}{2} < q < 1$ is that, for almost all choices of q , nonlinear interactions necessarily generate infinitely many modes on both critical circles (figure 1c). This occurs because each vector on the outer circle is the sum of

two inner vectors, and in turn each of these inner vectors is the sum of two (different) outer vectors, and so on.

So, for $\frac{1}{2} < q < 1$, each mode on each circle will be influenced by two types of 3WI: one type involving interaction with a pair of modes from the other circle, and the second involving interaction with one mode from each circle. (There is also the usual interaction between three waves at 120° on a single circle.) To understand the effect of this multitude of nonlinear interactions (figure 1c), we write the pattern-forming field $U(x, y, t)$ as

$$U = \sum_{j=1, |\mathbf{k}_j|=1}^{\infty} z_j(t) e^{i\mathbf{k}_j \cdot \mathbf{x}} + \sum_{j=1, |\mathbf{q}_j|=q}^{\infty} w_j(t) e^{i\mathbf{q}_j \cdot \mathbf{x}} + \text{h.o.t.},$$

where t is the time-scale for the slow evolution of the amplitudes, and the sums are over all modes on the two circles. In order to quantify the four coefficients that govern the two types of 3WIs, we write down archetypal equations (at lowest order) for the two different types of 3WI, first involving a triad of wavevectors \mathbf{k}_1 , \mathbf{k}_2 and $\mathbf{q}_1 = \mathbf{k}_1 + \mathbf{k}_2$, with amplitudes z_1 , z_2 and w_1 :

$$\begin{aligned} \dot{z}_1 &= \mu z_1 + Q_{zw} \bar{z}_2 w_1 + \text{cubic terms}, \\ \dot{z}_2 &= \mu z_2 + Q_{zw} \bar{z}_1 w_1 + \text{cubic terms}, \\ \dot{w}_1 &= \nu w_1 + Q_{zz} z_1 z_2 + \text{cubic terms}, \end{aligned} \quad (1)$$

where μ and ν are growth rates corresponding to wavenumbers 1 and q , and Q_{zw} and Q_{zz} are coefficients of the quadratic terms. Cubic terms play an important role in the dynamics of (1) [9], and their effect is included in the discussion below. We write similar equations for the second type of 3WI, involving the triad \mathbf{q}_2 , \mathbf{q}_3 and $\mathbf{k}_1 = \mathbf{q}_2 + \mathbf{q}_3$, with amplitudes w_2 , w_3 and z_1 :

$$\begin{aligned} \dot{w}_2 &= \nu w_2 + Q_{wz} \bar{w}_3 z_1 + \text{cubic terms}, \\ \dot{w}_3 &= \nu w_3 + Q_{wz} \bar{w}_2 z_1 + \text{cubic terms}, \\ \dot{z}_1 &= \mu z_1 + Q_{ww} w_2 w_3 + \text{cubic terms}, \end{aligned} \quad (2)$$

where Q_{wz} and Q_{ww} are two more quadratic coefficients.

These equations should be replicated for all possible combinations of modes from the two circles, whenever 3WI is possible. The evolution of this infinite set of waves could be exceedingly complicated, but we argue it is likely to be most strongly influenced by the outcome of the two types of 3WIs governed by (1) and (2). To this end, we summarize the results of [9] and others on equations (1) with appropriate cubic terms. Pure mode solutions are stable for ranges of values of μ and ν . The behavior of mixed solutions, where all three amplitudes are non-zero, is influenced heavily by the signs of the quadratic coefficients. If these have the same sign ($Q_{zz}Q_{zw} > 0$), there is a range of values of (μ, ν) where steady solutions of (1) with all three modes non-zero are stable. In contrast, if the quadratic coefficients have opposite sign ($Q_{zz}Q_{zw} < 0$), there is a range of values of (μ, ν) where there is time-dependent competition between the three amplitudes [9].

In a similar manner, in the multitude of 3WIs that occur when $\frac{1}{2} < q < 1$, the behavior of each type of 3WI will

depend on the products of the quadratic terms, $Q_{zz}Q_{zw}$ and $Q_{ww}Q_{wz}$ in (1) and (2), and will determine whether each type of interaction results in competition between modes or not. Consequently the signs of $Q_{zz}Q_{zw}$ and $Q_{ww}Q_{wz}$ will strongly influence the dynamics of the overall system. Specifically, if $Q_{zz}Q_{zw}$ and $Q_{ww}Q_{wz}$ are both negative, then we expect to find time-dependent competition leading to intermittent appearance of patterns with θ_z or θ_w , including the possibility of STC, with two full circles of modes present. Conversely, if $Q_{zz}Q_{zw}$ and $Q_{ww}Q_{wz}$ are both positive, only steady patterns are to be expected: these may be simple patterns such as stripes or hexagons, or they may have complex spatial structure, with a superposition of waves having a variety of orientations featuring the special angles θ_w and θ_z , possibly with patches of one pattern in a background of the other. In the intermediate case where, $Q_{zz}Q_{zw} > 0$ and $Q_{ww}Q_{wz} < 0$ (or the other way around), then resonant triad interactions involving θ_z are reinforced, while triads involving θ_w can be competitive (or vice-versa). In this case we expect to find steady superlattice patterns involving θ_z , or time-dependent competition between such superlattice patterns with different orientations.

We emphasise that these expectations for the overall behavior of the pattern-forming problem are based on the idea that the dynamics of any particular vector drawn from the infinite number of vectors on the two critical circles will be dominated by its linear growth rate and the 3WIs associated with the two types of triad to which that vector belongs.

There are two special values of the radius ratio q that do not immediately generate an infinite number of waves: when q is $\frac{1}{2}(\sqrt{5} - 1) = 0.6180$ or $\frac{1}{2}(\sqrt{6} - \sqrt{2}) = 0.5176$, corresponding to $\theta_z = 2\theta_w = 144^\circ$ and $\theta_z = 5\theta_w = 150^\circ$, only a finite number of wavevectors on the critical circles is generated. These two special cases correspond to 10-fold and 12-fold quasipatterns respectively (although an infinite set of vectors is generated in the 10-fold case once hexagonal interactions are included). The values of q that would lead to 8-fold patterns generate an infinite number of vectors. Hexagons and squares are also not exceptions: for example, if $q = 1/\sqrt{2}$, we have $\theta_w = 90^\circ$ but $\theta_z = 138.6^\circ$, which does not fit in a square lattice.

Considering both types of 3WIs provides an explanation of some of the observed Faraday wave phenomena in the experiments of [3]. These use the three-frequency forcing $f(t) = a_m \cos(m\omega t) + a_n \cos(n\omega t + \phi_n) + a_p \cos(p\omega t + \phi_p)$, where $(m, n, p) = (4, 5, 2)$ and $(6, 7, 2)$. The 3WIs are between harmonic modes, driven by the $(4, 2)$ and $(6, 2)$ components of the forcing, with the primary instability being to the larger frequency. The radius ratios are $q \approx 0.52$ and $q \approx 0.38$ in the two cases: these are the radius ratios that arise in 12-fold quasipatterns and 22° superlattice patterns. The presence of these two patterns as a function of the phases (ϕ_5, ϕ_2) and (ϕ_7, ϕ_2) is indicated by light areas in figure 2(a,b). The slopes of the bands and their periodicity are related to time translation symmetries of components of $f(t)$ [6].

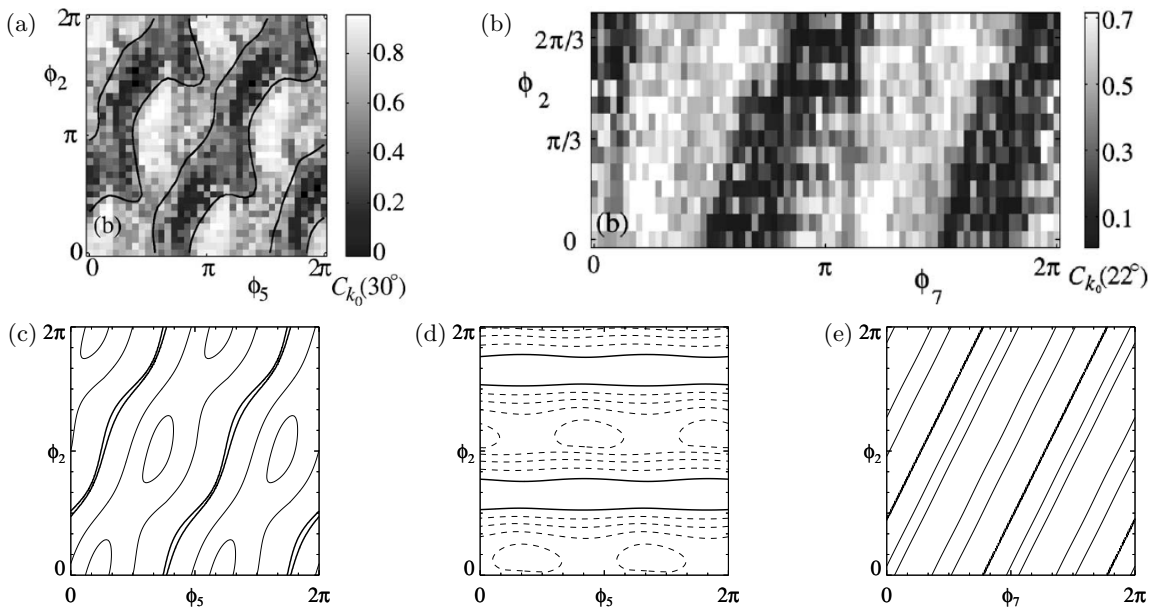


FIG. 2: (a,b) Experimental results of Ding and Umbanhowar [3], reproduced with permission. (a) The 30° angular autocorrelation function with (4, 5, 2) forcing: white indicates 12-fold quasipatterns, as a function of (ϕ_5, ϕ_2) . Black indicates disordered patterns. (b) The 22° angular autocorrelation function with (6, 7, 2) forcing: white indicates 22° superlattice patterns, as a function of (ϕ_7, ϕ_2) . (c,d,e) Products of quadratic coefficients. (c,d) Parameter values as in the experiment in (a), with (c) $Q_{zz}Q_{zw}$ (contours in steps of 0.2) and (d) $Q_{ww}Q_{wz}$ (contours in steps of 0.05) (e) Parameter values as in (b), showing $Q_{zz}Q_{zw}$ (contours in steps of 0.1). In all cases, the thick line is the zero contour, solid (dashed) lines are positive (negative) contours. In (c,e), $Q_{zz}Q_{zw}$ is negative only in very narrow diagonal bands; in (d), $Q_{ww}Q_{wz}$ is positive in two horizontal bands.

The two cases, (4, 5, 2) and (6, 7, 2) excitation, differ in that in the first case, $q > \frac{1}{2}$, and ‘two-way’ 3WIs between the different critical modes is possible, whereas in the second case, $q < \frac{1}{2}$, and no such two-way 3WIs can occur. We have calculated the values of the relevant quadratic coefficients using weakly nonlinear analysis of the Navier–Stokes equations for the experimental parameters by extending the method in [10]. In figure 2(c,d), we show $Q_{zz}Q_{zw}$ and $Q_{ww}Q_{wz}$ for the (4, 5, 2) case. Both products can take either positive or negative values, although each is dominated by one sign. In figure 2(e), we show $Q_{zz}Q_{zw}$ for the (6, 7, 2) case. Comparing with the experimental results in figure 2(a,b), we note that regions of 12-fold quasipatterns and 22° superlattice patterns correlate extremely well with regions of positive $Q_{zz}Q_{zw}$. Conversely, when $Q_{zz}Q_{zw}$ is small or negative, the autocorrelation function in the experiments is low and STC is seen [11]. The extra structure in figure 2(a), where the dark stripes broaden horizontally just above $\phi_2 = \frac{\pi}{2}$ and $\frac{3\pi}{2}$, is aligned with changes in $Q_{ww}Q_{wz}$ in figure 2(d), although our expectation would be for enhanced STC where $Q_{ww}Q_{wz}$ is negative.

There is clearly scope for further investigation of the role of the two-way 3WIs in this and other experiments, motivated by the encouraging alignment between the experimental autocorrelation functions and the calculated quadratic coefficients.

We have further investigated the importance of the signs of the quadratic coefficients in the two-way 3WIs

by devising a new model PDE for a field $U(x, y, t)$:

$$\frac{\partial U}{\partial t} = \mathcal{L}(\mu, \nu)U + Q_1 U^2 + Q_2 U \nabla^2 U + Q_3 |\nabla U|^2 - U^3. \quad (3)$$

The model (3) is an extension of those of [12], modified to allow the growth rates of two critical modes to be controlled independently. The linear part of the PDE \mathcal{L} acts on a mode e^{ikx} with eigenvalue $\sigma(k)$. The dependence of the eigenvalue on k is specified by $\sigma(1) = \mu$ and $\sigma(q) = \nu$, controlling the growth rates of the modes of interest; $\sigma'(1) = \sigma'(q) = 0$; and $\sigma(0) = \sigma_0 < 0$, controlling the depth of the minimum between $k = 1$ and $k = q$. With σ an even function of k , these requirements lead to a fourth-order polynomial in k^2 :

$$\sigma(k) = \frac{k^2 (A(k)\mu + B(k)\nu)}{q^4(1 - q^2)^3} + \frac{\sigma_0}{q^4}(1 - k^2)^2(q^2 - k^2)^2,$$

where $A(k) = (k^2(q^2 - 3) - 2q^2 + 4)(q^2 - k^2)^2 q^4$ and $B(k) = (k^2(3q^2 - 1) + 2q^2 - 4q^4)(1 - k^2)^2$. The linear operator \mathcal{L} is obtained by replacing k^2 by $-\nabla^2$. The nonlinear terms in the PDE model are simple quadratic and cubic combinations of U and its derivatives. Standard weakly nonlinear theory gives the values of Q_{zz} , Q_{zw} , Q_{ww} and Q_{wz} : having the three quadratic terms in (3) enables different sign combinations to be chosen in the amplitude equations (1) and (2).

Simulations of equation (3), carried out on a 30×30 domain for a range of (μ, ν) , are shown in figure 3(a) for $q = 0.66$ and values of Q_1 , Q_2 and Q_3 that give

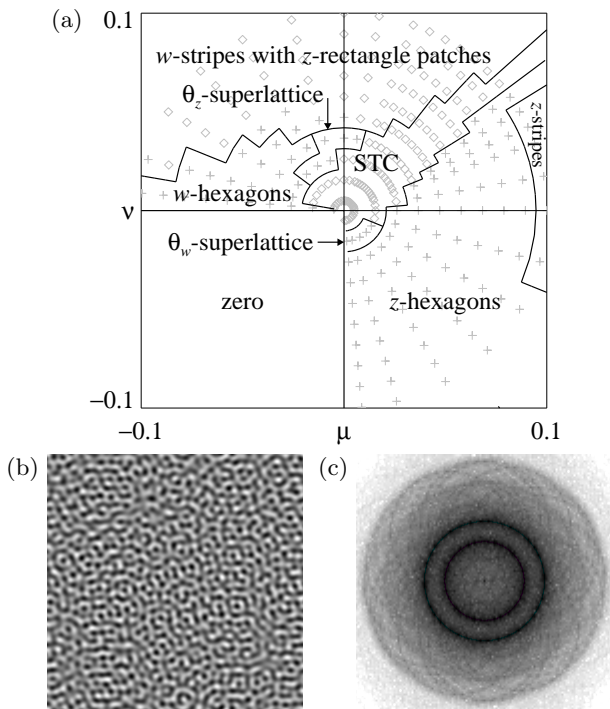


FIG. 3: (a) Bifurcation set showing the patterns that are seen for $q = 0.66$, $\sigma_0 = -2$, $Q_1 = 0.3$, $Q_2 = 1.3$, $Q_3 = 1.7$ (so $Q_{zz}Q_{zw} < 0$ and $Q_{ww}Q_{wz} < 0$). We find z -hexagons ($k = 1$), w -hexagons ($k = q$), spatio-temporal chaos (STC), mixed patterns (w -strips with patches of z -rectangles) and two types of superlattice pattern: one with 6 modes on the outer circle and 12 on the inner, separated by θ_w , and the other with 6 modes on the inner circle and 12 on the outer, separated by θ_z . Steady (time-dependent) patterns are indicated with a + (\diamond). The (μ, ν) scale is not uniform. (b) Pattern for parameters in the STC region, with $\mu = \nu = 0.00707$. The correlation length of this pattern is about 1–2 wavelengths. (c) The two critical circles are clearly seen in its power spectrum.

$Q_{zz}Q_{zw} < 0$ and $Q_{ww}Q_{wz} < 0$. We find a variety of patterns and STC, with a typical solution shown in figure 3 (b,c). For other choices of q and the quadratic

coefficients, the behavior of the PDE is broadly in line with the expectations. When $q < \frac{1}{2}$, we find no examples of STC. For $q > \frac{1}{2}$, we find steady and time-dependent patterns with many modes on both critical circles. In general, with both $Q_{zz}Q_{zw}$ and $Q_{ww}Q_{wz}$ positive, these patterns are all steady; time dependence (chaos or STC) is much more common when both $Q_{zz}Q_{zw}$ and $Q_{ww}Q_{wz}$ are negative. We find steady and time-dependent quasi-patterns only with the special values $q = 0.5176$ and $q = 0.6180$. Further details will be presented elsewhere.

We conclude that whenever there are 3WIs between waves on two critical circles with radius ratio between $\frac{1}{2}$ and 2, interactions in both directions must be taken into account. This is generic: these two-way 3WIs will be important in any problem with two comparable length scales. Most values of $q > \frac{1}{2}$ lead to the possibility of generating an infinite number of interacting waves. The exceptions are those values associated with 10- and 12-fold quasipatterns. The outcome of the 3WIs will be influenced by the signs of the quadratic coefficients in (1) and (2), with time-dependence and STC most likely in the case of both pairs of quadratic coefficients having opposite sign. These ideas have been confirmed in numerical investigations of a model PDE (3). By computing quadratic coefficients from the Navier–Stokes equations, we have shown that these ideas are in broad agreement with the experimental results of [3]: as the phases in the forcing are varied, switches between 12-fold quasipatterns or 22° superlattice patterns and STC line up with changes of sign of the products of quadratic coefficients.

Acknowledgments

We acknowledge valuable conversations with Yu Ding, Jay Fineberg, Paul Umbanhowar and Jorge Viñals, as well as comments from the referees. MS is grateful for support from the National Science Foundation (DMS-0709232).

-
- [1] H. Arbell and J. Fineberg, *Phys. Rev. E* **65**, 036224 (2002); T. Epstein and J. Fineberg, *Phys. Rev. Lett.* **92**, 244502 (2004); T. Epstein and J. Fineberg, *Phys. Rev. E* **73**, 055302(R) (2006); A. Kudrolli, B. Pier, and J. P. Gollub, *Physica D* **123**, 99 (1998).
 - [2] W. S. Edwards and S. Fauve, *J. Fluid Mech.* **278**, 123 (1994).
 - [3] Y. Ding and P. Umbanhowar, *Phys. Rev. E* **73**, 046305 (2006).
 - [4] I. Berenstein, M. Dolnik, L. Yang, A. M. Zhabotinsky, and I. R. Epstein, *Phys. Rev. E* **70**, 046219 (2004).
 - [5] T. Ackemann and T. Lange, *Appl. Phys. B* **72**, 21 (2001); M. A. Vorontsov and B. A. Samson, *Phys. Rev. A* **57**, 3040 (1998).
 - [6] J. Porter, C. M. Topaz, and M. Silber, *Phys. Rev. Lett.* **93**, 034502 (2004).
 - [7] W. B. Zhang and J. Viñals, *Phys. Rev. E* **53**, R4283 (1996).
 - [8] J. L. Rogers, W. Pesch, O. Brausch, and M. F. Schatz, *Phys. Rev. E* **71**, 066214 (2005); A. M. Rucklidge and M. Silber, *SIAM J. Appl. Dynam. Syst.* **8**, 298 (2009); C. M. Topaz, J. Porter, and M. Silber, *Phys. Rev. E* **70**, 066206 (2004).
 - [9] J. Guckenheimer and A. Mahalov, *Physica D* **54**, 267 (1992); J. Porter and M. Silber, *Physica D* **190**, 93 (2004).
 - [10] A. C. Skeldon and G. Guidoboni, *SIAM J. Appl. Math.* **67**, 1064 (2007).
 - [11] Y. Ding, *Personal communication*.
 - [12] J. Swift and P. C. Hohenberg, *Phys. Rev. A* **15**, 319 (1977); R. Lifshitz and D. M. Petrich, *Phys. Rev. Lett.* **79**, 1261 (1997).